



GNSS Solar Astronomy in real-time during more than one solar cycle

Manuel Hernández-Pajares^{a,b,*}, Alberto García-Rigo^{b,a}, Enric Monte-Moreno^c,
 Qi Liu^{d,a}, David Roma-Dollase^{b,a}, Heng Yang^{e,a}, Yannick Béniguel^f,
 David Moreno-Borràs^a, Octavi Fors^g, Haixia Lyu^{h,a}, Raul Orus-Perezⁱ,
 Javier Ventura-Traveset^j

^aUPC-IonSAT, Mod. C3 Campus Nord UPC, Barcelona 08034, Spain

^bIEEC, Ed.Nexus Campus Nord UPC, Barcelona 08034, Spain

^cUPC-TALP, Mod. D5 Campus Nord UPC, Barcelona 08034, Spain

^dCollege of Geography and Environmental Science, Henan University, Kaifeng 475004, China

^eSchool of Electronic Information and Engineering, Yangtze Normal University, Chongqing 408100, China

^fInformatique, Electromagnétisme, Electronique, Analyse numérique, IEEA, Courbevoie 92400, France

^gDept. Física Quàntica i Astrofísica, Institut de Ciències del Cosmos (ICCUB), Universitat de Barcelona,

IEEC-UB, Martí i Franquès 1, Barcelona 08028, Spain

^hGNSS Research Center, Wuhan University, Wuhan 430079, China

ⁱESA, ESTEC, Noordwijk, 2201 AZ, The Netherlands

^jESA, Centre Spatial de Toulouse, Toulouse 31000, France

Received 29 June 2023; received in revised form 4 December 2023; accepted 6 December 2023

Abstract

This work presents a summary of the continuous non-stop (hereinafter 24/7) real-time measurement and warning system for EUV solar activity, which is based on worldwide multifrequency Global Navigation Satellite Systems (GNSS) observations. The system relies on continuous tracking of the intensity of expected global patterns in the Earth's ionosphere's free electron distribution, which are associated with solar flares. The paper includes a discussion on the foundations of GNSS Solar Astronomy, along with details on its real-time implementation that began in 2011. Furthermore, a summary of the corresponding validation is provided, comparing it to external and direct solar EUV flux measurements obtained from SOHO-SEM. Finally, there will be a brief mention of the ongoing efforts to extend this technique to detect huge extra-solar sources.

© 2023 Published by Elsevier B.V. on behalf of COSPAR.

Keywords: Solar astronomy; Global navigation satellite systems; Ionosphere; Solar flares

1. Introduction

GNSS Solar Astronomy refers to the measurement and warning system for monitoring the EUV flux activity of the Sun. This system relies on worldwide multifrequency

Global Navigation Satellite Systems (GNSS) observations to track the corresponding response of the Earth's ionosphere. Pioneering works in this field were presented at the beginning of the century (Afraimovich (2000), García-Rigo et al. (2007)). About a decade ago, a mature version of the technique became available (Hernández-Pajares et al. (2012)), coinciding with its implementation and continuous real-time application at UPC-IonSAT facilities under the ESA-funded MONITOR project (Béniguel

* Corresponding author at: UPC-IonSAT, Mod. C3 Campus Nord UPC, Barcelona 08034, Spain.

E-mail address: manuel.hernandez@upc.edu (M. Hernández-Pajares).

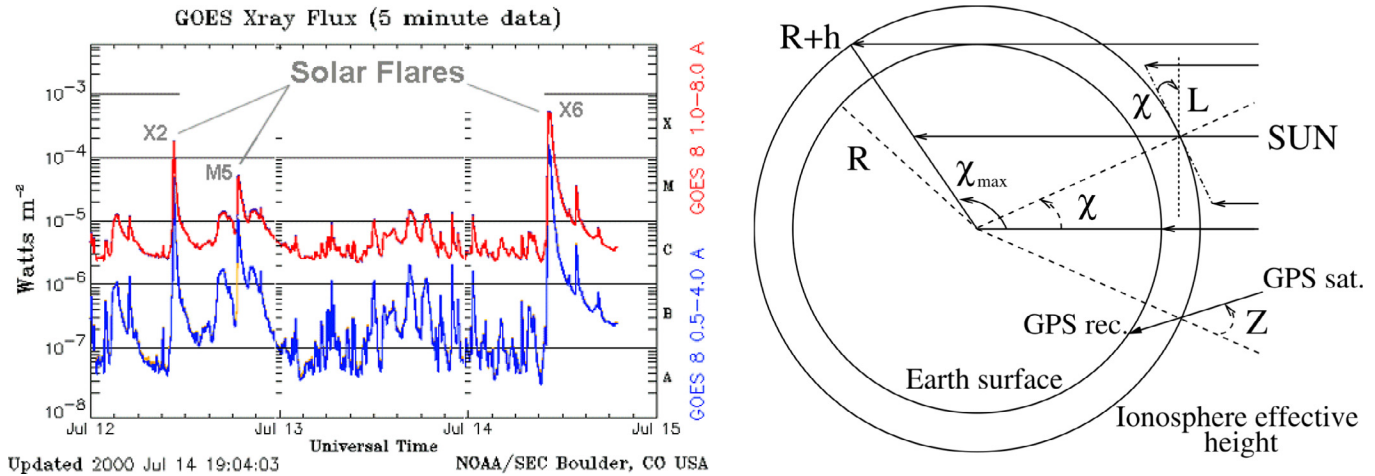


Fig. 1. Left-hand plot: Example of solar X-ray flux measurements from GOES spacecraft during solar flares on 12–July 14, 2000, extracted from <https://spaceweather.com/glossary/flareclasses.html>; right-hand plot: layout summarizing the solar flare geoeffectiveness geometry (extracted from Hernández-Pajares et al. (2012)).

et al. (2017)). The system operates with a time resolution of 30 s.

The consistency between indirect solar EUV flux rate measurements provided by GNSS and direct conventional EUV flux measurements from instruments onboard solar probes, such as SOHO-SEM and GOES15-EUVS, is demonstrated in the work by Singh et al. (2015). This study shows the strong agreement with the simple first-principles based model of GNSS Ionosphere (Hernández-Pajares (2022)), which supports GNSS Solar Astronomy. As a result, the new technique was able to accurately characterize the statistical nature of solar flare occurrences by itself (Monte-Moreno and Hernández-Pajares (2014)). The operational implementation of this technique began in 2011 and has been continuously applied since 2014 without significant interruptions.

The paper is organized as follows: after this introduction, the next section provides a summary of the first-principle based model that supports GNSS Solar Astronomy. Following that, the coverage of the RT GNSS Solar Astronomy conducted thus far, along with the validation against the newly available direct measurements of solar EUV flux in the [26,34]nm range from SOHO-SEM¹, will be summarized in the subsequent section. The conclusions will encompass an executive summary, including the ongoing efforts to extend this technique to extremely powerful extra-solar active EUV sources. These efforts aim to facilitate general real-time GNSS Astronomy in the near future.

2. First principles based model of GNSS Solar Astronomy

A solar flare is an exceptionally powerful energy explosion on the Sun that produces a wide range of electromagnetic waves, spanning from radio waves to EUV, X-ray,

and γ -ray radiation. These flares occur when the energy stored in twisted magnetic fields, typically located above sunspots, is suddenly released. Solar flares are classified based on their X-ray flux in the [1,8]Å range², with distinctions between major, mid, and small flares (referred to as X, M, and C-class flares, respectively; see Fig. 1).

2.1. SOLERA model: Method for the estimation of the EUV flux rate

In this section, we present a relationship between the variations of electron content in the ionosphere and variations in the EUV flux. This relationship is derived from first principles and demonstrates an affine dependence, specifically taking the form of $y = ax + b$.

Let's consider the expected extraordinary rate of change of Vertical Total Electron Content (referred to as V or VTEC, as described in Hernández-Pajares et al. (2011)) in the Earth's ionosphere due to a solar flare, denoted as $\dot{V} \equiv \frac{\partial V}{\partial t}$. For a given solar-zenith angle χ , which corresponds to the Ionospheric Pierce Point (IPP) of the VTEC measurement, the rate of change \dot{V} can be related to the rate of change in the source solar EUV flux, denoted as \dot{I} , through a projection function C. This relationship takes into account the geo-effectiveness of the considered spectral range, denoted as η . Further details and the graphical representation can be found in the right plot of Fig. 1 and in Hernández-Pajares et al. (2012).

$$\dot{V} = \eta' \cdot C(\chi) \cdot \dot{I} \rightarrow \frac{\partial V}{\partial t} = a(t) \cos \chi + b(t) \quad (1)$$

where each GNSS transmitter–receiver ionospheric combination of carrier phases, $L_l = L_1 - L_2$, provide a direct estimation of the VTEC rate as

¹ https://lasp.colorado.edu/eve/data_access/eve_data/lasp_soho_sem_data/long/15_sec_avg/year/

² https://www.esa.int/Science_Exploration/Space_Science/What_are_solar_flares+

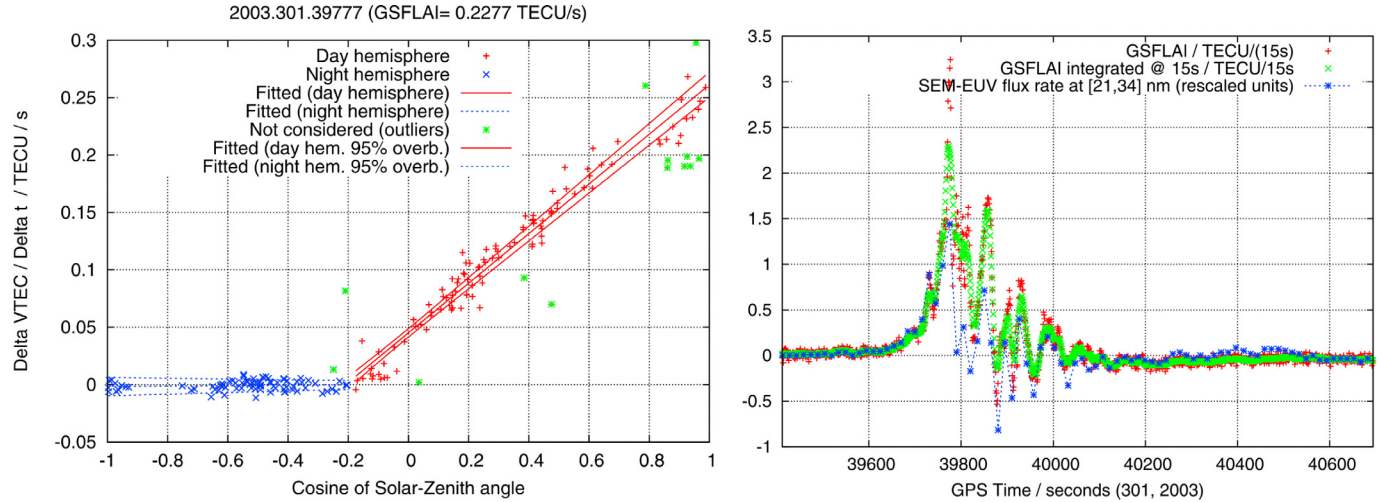


Fig. 2. Left-hand plot: Detrended VTEC rate, \dot{V} , vs cosine of solar-zenithal angle, $\cos \chi$, for a major solar flare and the associated ionospheric super-storm during October 28th, 2003, precursor flare of Halloween storm (X17.2 flare, day 301, 2003, 39777s of GPS time). Right-hand plot: GSFLAI results compared with SEM EUV flux rate at [21,34]nm band, \dot{E} , provided by SOHO during representative X-class solar flares, and rescaled as $0.502 \times \dot{E} / 1.5 \times 10^8 / \text{photons}/\text{cm}^2/\text{s}$ (extracted from Hernández-Pajares et al. (2012)).

$$\dot{V} = \frac{1}{M} \frac{dL_I}{dt} \quad (2)$$

Being M the ionospheric mapping function at the central time (Hernández-Pajares et al. (2011)), Eq. 1 straightforwardly shows that $a(t) + b(t)$ corresponds to the VTEC rate at the sub-solar point, primarily influenced by the geoeffective EUV flux rate associated with the flare (Singh et al. (2015)). This VTEC rate can be computed in the Sun-illuminated part of the ionosphere by estimating two global unknowns, a and b , at each given time t using the Least Squares method with the removal of outliers. These estimates are obtained from the available observational pairs $(\chi_j, \dot{V}_j)_{j=1, N_{obs}}$, which are directly measured at several ionospheric combinations of GNSS carrier phases, typically from over 100 ground GNSS receivers and + 10 GNSS transmitters simultaneously in view from each given receiver, every second (high-rate) or every 30 s. This results in a large dataset of + 100 million observations worldwide during a given (recent) day. An example of the VTEC dependence in the ionosphere associated with a solar flare is shown in the left plot of Fig. 2, following Eq. 3.

Another approach to solving Eq. 1 involves estimating only the unknown α after assuming that

$$\dot{V} \simeq \alpha \cdot \frac{\cos \chi + 0.2}{1 + 0.2} \quad (3)$$

In this context, it is observed that $b \simeq 0.2 \cdot a$, and $\alpha = a(1 + 0.2)$ represents the sub-solar flux rate. This value, α , is directly estimated as a single unknown per time in this approximation. This empirical relationship, depicted in Fig. 1 of Singh et al. (2015), is associated with the typical effective height of a few hundred kilometers at which overionization occurs. With the SOLAR Euv flux RATE GNSS proxy (SOLERA) term (also known as GNSS Solar Flare

Activity Indicator, GSFLAI, see Hernández-Pajares et al. (2012)), we will refer to any of these direct estimations, either $a(t) + b(t)$ or $a(t)$, and it encompasses both one- or two-unknown-per-epoch models.

Let's revisit the example that illustrates the performance of the model in terms of the observed relationship between VTEC rate and the cosine of the solar-zenith angle, as depicted in the left plot of Fig. 2. The corresponding SOLERA measurement is represented by a single point in the right plot of Fig. 2, corresponding to a GPS Time of 39777 s. This measurement coincides with a major flare that occurred on day 301 of 2003, just before the Halloween geomagnetic storm. The validity of the measurement is confirmed for the entire time period by comparing it with SOHO SEM EUV flux rate measurements in the [21–34]nm range (for further details, please refer to Hernández-Pajares et al. (2012)).

Last but not least, in order to specifically detect significant increases in solar EUV flux, we will also examine the detrended VTEC at various time scales, denoted as δt .

$$\tilde{V}(t) = V(t) - \frac{V(t - \delta t) + V(t + \delta t)}{2} \quad (4)$$

(formally related to the drift rate, $\ddot{V} = -2\tilde{V}/\delta t$), the detrended VTEC can be analyzed using the SOLERA model, resulting in the computation of the corresponding SOLERAdrift index in Eq. 5, similar to Eq. 2 but with coefficients \tilde{a} and \tilde{b} referring to the detrended VTEC, instead of to the VTEC rate:

$$\tilde{V} = \eta' \cdot C(\chi) \cdot \tilde{I} \rightarrow \tilde{V} = \tilde{a}(t) \cos \chi + \tilde{b}(t) \quad (5)$$

Then we will refer to any of these direct estimations, adjusted in a similar way as a and b of Eq. 2, either $\tilde{a}(t) + \tilde{b}(t)$ or $\tilde{a}(t)$, as SOLERAdrift index.

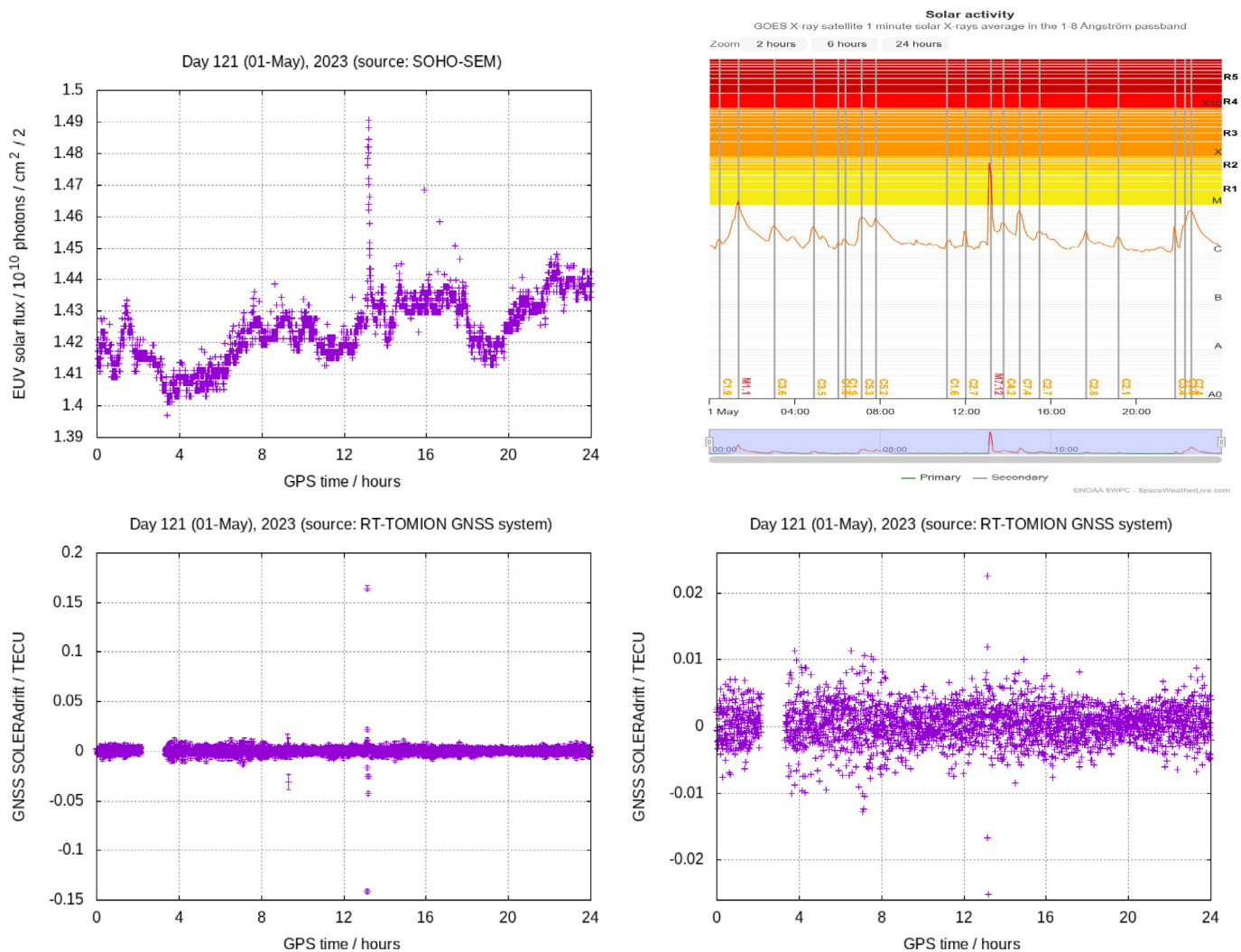


Fig. 3. Top-left plot: Direct EUV flux measurements at [21–34]nm provided by SOHO-SEM probe vs GPS time, in seconds of day 121 (01-May) 2023 (https://lasp.colorado.edu/eve/data_access/eve_data/lasp_soho_sem_data/long/15_sec_avg/2023/23_05_01_v4.00). Top-right plot: The corresponding X-band solar flux at [1,8]Å measured by GOES (<https://www.spaceweatherlive.com/en/archive/2023/05/01/xray.html>). Bottom left plot: GNSS SOLERA drift estimation (<http://chapman.upc.es/monitor/2023/121/NRT/SOLERA-drift/>), and the corresponding vertical zoom, after removing the three estimations with error greater than 0.005 TECU.

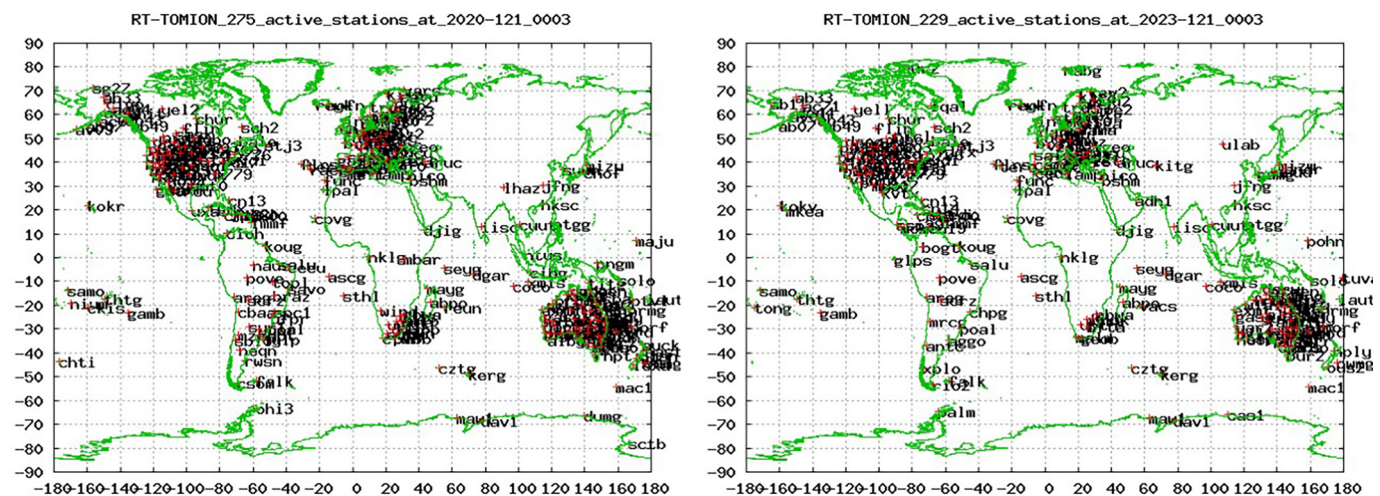


Fig. 4. The available GNSS receivers in real-time at 00h03m GPS time, during the same day 121 at 00h03m, of years 2020 (left) and 2023 (right).

A recent example of the time evolution of SOLERAdrift, extracted from our RT-TOMION system,

<http://chapman.upc.es/monitor/2023/121/NRT/SOLERA-drift/> on May 1st, 2023 (day 121), is shown in the bottom left plot of Fig. 3. A closer view of the smaller SOLERAdrift values, after excluding three estimations with errors greater than 0.005 TECU, can be seen in the bottom right plot. This can be compared with the direct SOHO-SEM EUV flux measurements at [21–34] nm, which are presented in the top left plot of the same figure. Additionally, the top right plot displays the X-ray band solar flux with much higher precision. It is noteworthy that the RT-SOLERAdrift at 30 s demonstrates high sensitivity, successfully detecting not only M-class (mid-

intensity) flares but also a significant portion of C-class (low-intensity) flares, consistent with our previous studies (Singh et al. (2015)).

3. RT GNSS Solar Astronomy coverage and validation

Since the start of the 24/7 service for RT GNSS Solar Astronomy, over 11,000,000 SOLERAdrift estimations have been conducted, at a frequency of once every 30 s, spanning more than one solar cycle (+11 years). The availability of GNSS receivers in real-time is dynamic and can undergo slight changes within a given day. Moreover, it can vary more significantly between different epochs, as illustrated in Fig. 4.

The histogram of SOLERAdrift values, presented in a semilog scale (see Fig. 5), clearly shows the tail of the distribution. It reveals values of up to approximately 0.2 TECU, which correspond to the occurrence of major solar flares, as exemplified in the recent example depicted in Fig. 3, where the values surpass the threshold of 0.15 TECU coinciding with the most intense M7.12 solar flare happening this day. Other flares during this day, beyond the ones automatically detected and warned by our 24/7 RT system when —SOLERAdrift— is larger than 0.02 TECUs, are also seen: around 15 h, coinciding with an C7.4 weak flare, around 23.5 h, another C7.4 weak flare, and around 07 h in agreement with a C5.3 solar flare (see Fig. 3).

In terms of a new validation check, the left plot of Fig. 6 compares the detrended direct EUV flux measurements provided by SOHO with the GNSS SOLERAdrift estimation since 2020, focusing on major events that are less affected by the increased noise resulting from the discretization of the current SOHO-SEM EUV measurements (as seen in the top-left plot of Fig. 3, and the reason to show them directly, without detrending). The correlation

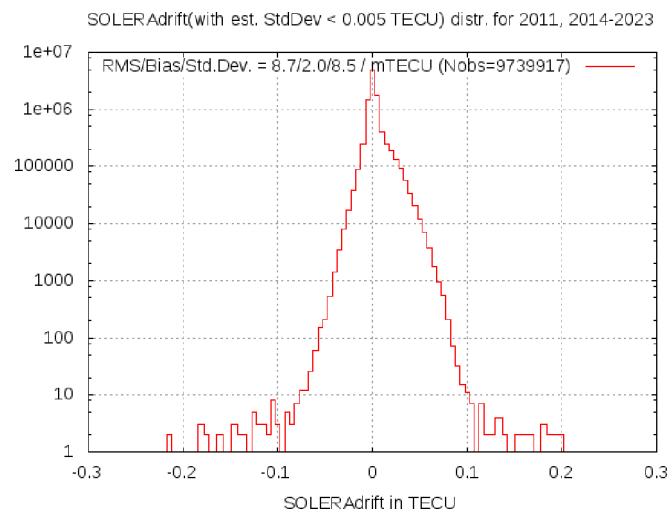


Fig. 5. Distribution of SOLERAdrift values for years 2011 and 2014–2023, when the estimated standard deviation of the error is smaller than 0.005 TECU and one single outlier in the whole period has been eliminated.

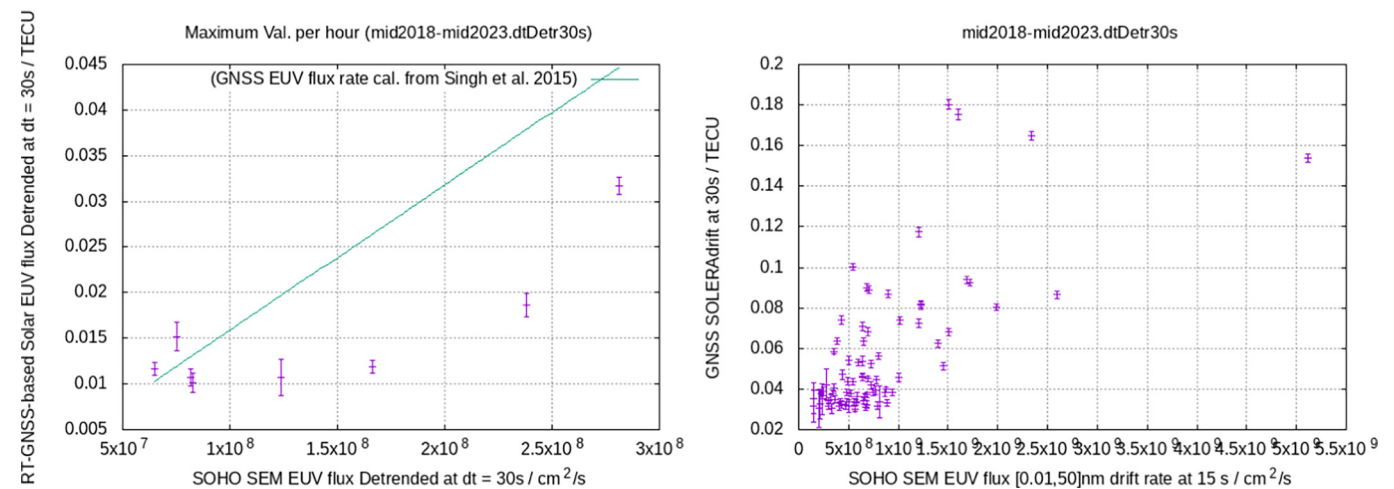


Fig. 6. In both plots we represent the most significant relationships of the SOLERAdrift index, computed in real-time and with a detrending time interval of 30 s, in TECUs, vs the detrended EUV SOHO-SEM observations (in photons per squared cm and second) within the spectral range of [26,34]nm detrended at a time interval of 30 s (left plot), and vs the detrended EUV SOHO-SEM observations in the same units within the spectral range of [0.01,50] nm and detrended at a time interval of 15 s (right plot).

observed is quantitatively consistent with previous studies, such as Singh et al. (2015). To mitigate the impact of discretization noise in the SOHO SEM measurements, an alternative approach is to compare SOLERAdrift with flux rate drift, i.e. detrended, measurements in a wider spectral band ([0.01, 50]nm), benefiting from higher count numbers (as shown in the right plot of Fig. 6). However, it is important to acknowledge the potential risk of saturation in the measurements during major flares.

4. Conclusions

The RT GNSS Solar Astronomy product, known as SOLERAdrift, which has been computed in real-time by UPC-IonSAT since 2011, is presented in this work. It demonstrates good performance, exhibiting sensitivity to major, mid, and small solar flares, with a time resolution of 30 s. This achievement has been made possible by leveraging the real-time GNSS facilities resulting from the international collaborative effort in GNSS Ionosphere (Hernández-Pajares et al. (2009)), which has been extended to real-time service (Caissy et al. (2012), Liu et al. (2021)). The evolution of this GNSS Solar Astronomy service could involve expanding its capabilities to detect and measure extremely powerful extra-solar sources. This possibility may become feasible as the initial evidence of the viability of GNSS Astronomy (Hernández-Pajares and Moreno-Borràs (2020)) is further substantiated by a new technique with enhanced sensitivity, which can also be applied in real-time conditions 24/7.

Declaration of Competing Interest

The authors declare that they have no known competing financial interests or personal relationships that could have appeared to influence the work reported in this paper.

Acknowledgments

This work has been supported by the projects MONITOR (funded by ESA/ESTEC in 2010, Contract No. 4000100988, and by ESA/EGNOS project office in 2014) and GNSS Astronomy (ESA/ESTEC Contract No.

4000133257/20/NL/GLC in 2021). This paper has been performed coinciding with the execution of PITHIA-NRF H2020 project (H2020-INFRAIA-2018–2020101007599).

References

- Afraimovich, E., 2000. Gps global detection of the ionospheric response to solar flares. *Radio Sci.* 35 (6), 1417–1424. <https://doi.org/10.1029/2000RS002340>.
- Béniguel, Y., Cherniak, I., Garcia-Rigo, A., et al., 2017. Monitor ionospheric network: two case studies on scintillation and electron content variability. *Ann. Geophys.*, volume 35. Copernicus GmbH, p. 377. <https://doi.org/10.5194/angeo-35-377-2017>.
- Caissy, M., Agrotis, L., Weber, G., et al., 2012. The international gnss real-time service. *GPS World* 6 (23), 52–58.
- García-Rigo, A., Hernández-Pajares, M., Juan, J., et al., 2007. Solar flare detection system based on global positioning system data: First results. *Adv. Space Res.* 39 (5), 889–895. <https://doi.org/10.1016/j.asr.2006.09.031>.
- Hernández-Pajares, M., 2022. Gnss ionosphere. In: Sideris, Michael G. (Ed.), *Encyclopedia of Geodesy*. Springer International Publishing, New York City, pp. 1–7. https://doi.org/10.1007/978-3-319-02370-0_172-1.
- Hernández-Pajares, M., García-Rigo, A., Juan, J.M., et al., 2012. Gnss measurement of euv photons flux rate during strong and mid solar flares. *Space Weather* 10 (12), 1–16. <https://doi.org/10.1029/2012SW000826>.
- Hernández-Pajares, M., Juan, J., Sanz, J., et al., 2009. The IGS VTEC maps: a reliable source of ionospheric information since 1998. *J. Geodesy* 83 (3–4), 263–275. <https://doi.org/10.1007/s00190-008-0266-1>.
- Hernández-Pajares, M., Juan, J.M., Sanz, J., et al., 2011. The ionosphere: effects, GPS modeling and the benefits for space geodetic techniques. *J. Geodesy* 85 (12), 887–907. <https://doi.org/10.1007/s00190-011-0508-5>.
- Hernández-Pajares, M., Moreno-Borràs, D., 2020. Real-time detection, location, and measurement of geoeffective stellar flares from global navigation satellite system data: New technique and case studies. *Space Weather* 18 (3). <https://doi.org/10.1029/2020SW002441>, e2020SW002441.
- Liu, Q., Hernández-Pajares, M., Yang, H., et al., 2021. The cooperative igs rt-gims: a reliable estimation of the global ionospheric electron content distribution in real time. *Earth Syst. Sci. Data* 13 (9), 4567–4582. <https://doi.org/10.5194/essd-13-4567-2021>.
- Monte-Moreno, E., Hernández-Pajares, M., 2014. Occurrence of solar flares viewed with gps: statistics and fractal nature. *J. Geophys. Res.: Space Phys.* 119 (11), 9216–9227. <https://doi.org/10.1002/2014JA020206>.
- Singh, T., Hernández-Pajares, M., Monte, E., et al., 2015. Gps as a solar observational instrument: Real-time estimation of euv photons flux rate during strong, medium, and weak solar flares. *J. Geophys. Res.: Space Phys.* 120 (12), 1–11. <https://doi.org/10.1002/2015JA021824>.